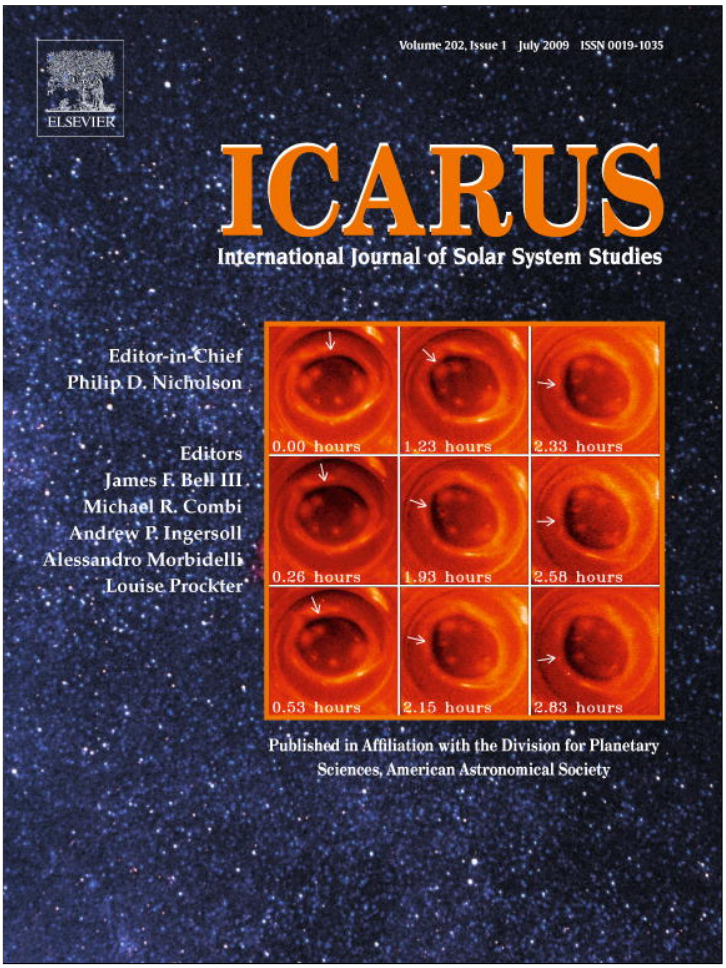

Icarus 202 (2009) 90–94

Contents lists available at ScienceDirect

Icarus

www.elsevier.com/locate/icarus

Seasonal and inter-annual changes of volume density of martian CO_2 snow from time–variable elevation and gravity

Koji Matsuo, Kosuke Heki *

Dept. Natural History Sci., Hokkaido University, N10 W8, Kita-ku, Sapporo-City, Hokkaido 060-0810, Japan

ARTICLE INFO

Article history:
Received 9 October 2008
Revised 5 February 2009
Accepted 26 February 2009
Available online 5 March 2009

ABSTRACT

The martian atmosphere seasonally exchanges CO_2 with the surface by repeating condensation and sublimation, causing seasonal growth and decay of the polar CO_2 snowcaps. These processes leave two kinds of geodetic signatures, i.e. seasonal changes of the martian gravity field and of surface elevation of the snow-covered regions. Here we study gradual increase of the volume density of the martian snow due to compaction, by combining these two data sets during 1999–2001 covering three martian winters. We found that light fresh snow of $\sim 0.1 \times 10^3$ kg m^{-3} slowly becomes denser reaching $\sim 1.0 \times 10^3$ kg m^{-3} or more immediately before it thaws. The maximum snow density varies slightly from year to year, and between hemispheres. In the second southern winter, the density became as high as $\sim 1.6 \times 10^3$ kg m^{-3}. This might have been caused by a dust storm activity, e.g. increased mixing of silicate particles and/or enhancement of sintering.

1. Introduction

Ninety-five percent of the current atmosphere of Mars is carbon dioxide (CO_2). Up to one third of the total CO_2 is considered to solidify every martian year, i.e. it accumulates as "snow" in the polar region of the wintry hemisphere where temperature drops below the CO_2 condensation point. It sublimates into atmosphere in late spring. Such seasonal mass redistribution can be measured by two independent geodetic techniques, i.e. altimetry and gravimetry.

The observations of topography by the Mars Orbiter Laser Altimeter (MOLA) on board the Mars Global Surveyor (MGS) spanned more than a full martian year. In addition to stationary topography, they revealed changes in the surface elevation in specific high-latitude (65.5–86.5 degrees) regions due to seasonal growth and decay of the polar snowcaps. Smith et al. (2001) collected over 66 million altitude data, and applied profile analysis to obtain a longitude-averaged data set with an accuracy of 5–6 cm. Increases of elevation more than a meter in winter hemispheres are clear there. Apart from that, Doppler tracking of the spacecraft revealed seasonal redistribution of CO_2 in terms of temporal changes of certain low degree Stokes' coefficients of the martian gravity field (Yoder et al., 2003; Konopliv et al., 2006).

Such seasonal altitude and gravity changes occur in phase, and we can compare the two quantities to infer average volume density of the polar snow packs. Smith et al. (2001), by comparing the MOLA surface altitude data with the changes of the martian oblateness (the J_2 component of the gravity field), estimated the average density of the snow as $(0.91 \pm 0.23) \times 10^3$ kg m^{-3}. This value is ~40% less than CO_2 ice ($\sim 1.5 \times 10^3$ kg m^{-3}). There they assumed that the snow density remains constant throughout the year.

In the Earth, water snow density is known to change in time; light freshly-fallen snow ($\sim 0.08 \times 10^3$ kg m^{-3}) often becomes as dense as 0.5×10^3 kg m^{-3} before spring thaw (e.g., Heki, 2004). Feldman et al. (2003) inferred the amount of the martian CO_2 snow by neutron spectrometry and compared it with the MOLA elevation results. They found that their results were often smaller than those inferred from altimetry data. Hence they suggested that snow density was, at that time, substantially lower than 0.91×10^3 kg m^{-3}, the value they assumed after Smith et al. (2001) in order to compare their snow weight data and the MOLA elevation changes. They speculated that the martian snow density might continuously increase due to compaction and re-crystallization. Here we try to reveal such temporal changes of snow density by combining the available elevation and gravity data sets.

2. Estimation of time–variable snow density

2.1. Gravimetric and altimetric ΔJ_3

We use the elevation (snow depth) changes from MOLA given in Fig. 2 of Smith et al. (2001). The differences of elevations from reference values, at 20 latitude bands from 65.5 to 86.5 degrees, are given at every 15 degrees in the solar longitudes L_s (L_s starts from the vernal equinox and changes by 360° in a martian year). Fig. 1 illustrates such snow depth snapshots between L_s 105° and

* Corresponding author. Fax: +81 11 706 3826.
E-mail address: heki@mail.sci.hokudai.ac.jp (K. Heki).

0019-1035/$ – see front matter
doi:10.1016/j.icarus.2009.02.023

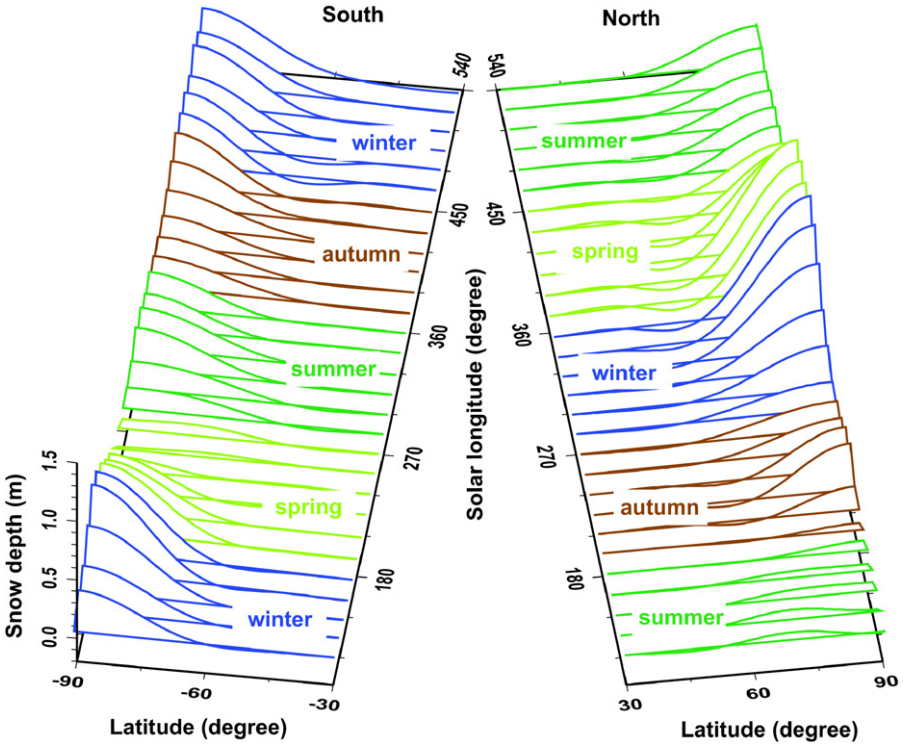

Fig. 1. Time series of changes in latitudinal profiles of snow depth at every 15 degrees of solar longitude L_s between 105° and 525° expressed as the sum of zonal spherical harmonics with degrees 2–10. The left and right panels show south and north regions, respectively. Snow depth attains the largest value (∼1.5 and ∼1.0 m in north and south regions, respectively) from late winter to early spring.

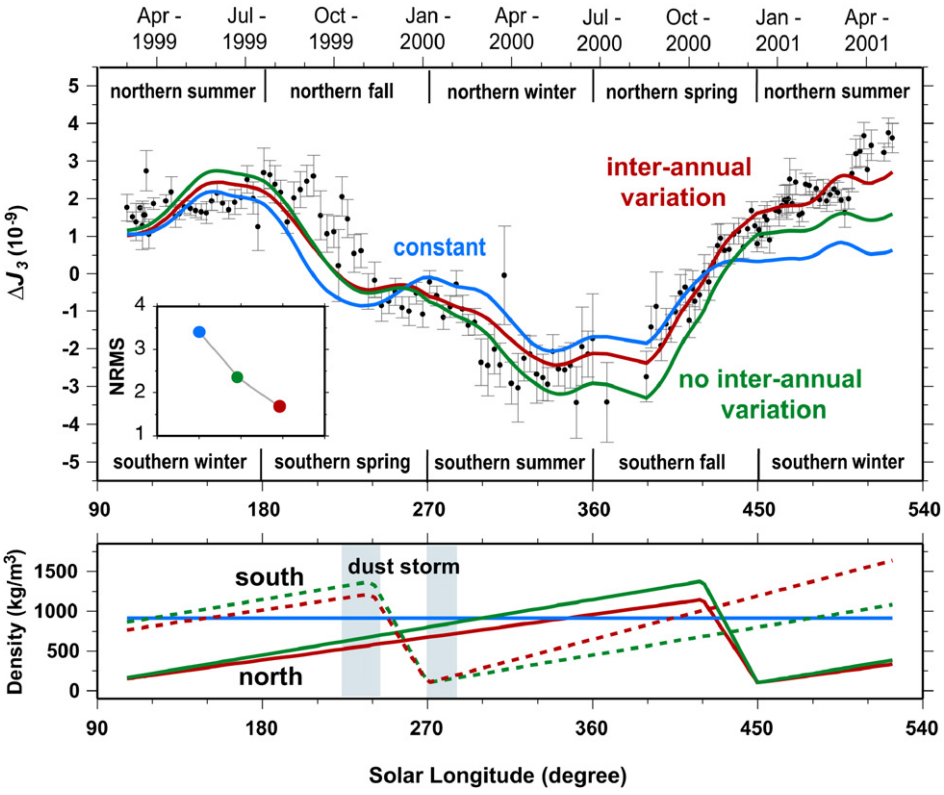

Fig. 2. (Upper panel) Time series of changes in gravity coefficient J_3 (ΔJ_3). The black dots with 1-σ error bars show gravimetric ΔJ_3 observed by MGS (Konopliv et al., 2006). The three curves show altimetric ΔJ_3 calculated from MOLA snow depth data (Smith et al., 2001), where the average density of snow pack is assumed constant (model 1, blue), time–variable without inter-annual difference (model 2, green), and time–variable with inter-annual difference (model 3, red). Improvement of normalized root-mean-squares (NRMS) of post-fit residuals is shown in the inset (their colors correspond to those of the curves). (Lower panel) Time series of average snow density in the northern (solid lines) and southern hemispheres (dashed lines). Three colors correspond to the three models shown in the upper panel. The two gray bars indicate regional dust storms (Smith, 2004), and the second one that started at $L_s \sim 270°$ in the south polar region may have increased the snow density in the second southern winter. (For interpretation of the references to color in this figure legend, the reader is referred to the web version of this article.)

525° expressed as the sum of zonal spherical harmonics with degrees up to 10. For the gravity data, we used the J_3 (a component representing "pear shape" of the planet) time series obtained by the Earth-based two-way Doppler measurements (the data shown in Fig. 10a of Konopliv et al., 2006). Because it is difficult to discriminate low degree odd zonal coefficients, such "ΔJ_3" actually represents the sum of contributions from changes in all odd zonal coefficients, δJ_3, δJ_5, $\delta J_7, \ldots$. Konopliv et al. (2006) gives the combination for the case of MGS as

$$\Delta J_3 \equiv \delta J_3 + 1.26\delta J_5 + 1.31\delta J_7 + 1.25\delta J_9 + \cdots. \quad (1)$$

Their "ΔJ_2" also represent the sum of contributions from all even zonal coefficients, $\delta J_2, \delta J_4, \delta J_6, \ldots$.

Both the "ΔJ_2" and "ΔJ_3" components are available as time–variable gravity coefficients in Konopliv et al. (2006). We here used only the "ΔJ_3" time series that are more suitable to explore asymmetric mass redistribution such as seasonal mass exchange between polar caps. Moreover, because MGS operates in a near polar orbit, odd zonal coefficients are more accurately determined, i.e., the signal to noise ratio of "ΔJ_3" in seasonal changes is ten times as good as that of "ΔJ_2" (Konopliv et al., 2006). We took out time span between 28 February 1999 and 25 May 2001 when both elevation and gravity data are available. Because the gravity and elevation data are not synchronously given, we interpolated the elevation data to obtain those at the same epochs as the gravity data using the third order spline function. It should be noted that we may have underestimated the formal errors of the snow densities discussed in the later sections because we did not consider errors of the interpolated elevation data. In this study, we scale the formal errors of the estimated parameters with post-fit residuals to get realistic errors.

The observed elevation change can be converted into change in J_n (altimetric δJ_n) by

$$\delta J_n = -\delta C_{n0} = \frac{3}{2a\rho_{\mathrm{ave}}(2n+1)} \int \Delta\sigma(\theta,\phi)\bar{P}_{n0}(\sin\theta)\cos\theta\, d\theta, \quad (2)$$

where a and ρ_{ave} are the martian radius and average density, and $\Delta\sigma$ is the surface mass (i.e. snow volume multiplied by its average density ρ_{snow}) at latitude θ and longitude ϕ over a unit area (Wahr et al., 1998). The integration is performed over the entire martian surface, and we get "ΔJ_3" (we simply refer to this as ΔJ_3 hereafter) by combining calculated coefficients using Eq. (1). There we neglected coefficients with degrees higher than 9 because their coefficients are not given in Eq. (1) (Konopliv et al., 2006). Although they are generally small (e.g., δJ_{11} is ~10% of ΔJ_3), they tend to have the same sign as the lower degree coefficients and this neglect may cause overestimate of the snow density by up to 20% if coefficients for higher terms are similar to those in Eq. (1). This, however, hardly affects the discussion on temporal density changes, the main target of the study.

By comparing the gravimetric ΔJ_3 and the altimetric ΔJ_3, we can estimate the average density of the snow. First, we assumed that this density does not depend on time (model 1). The blue curve in Fig. 2 shows the altimetric ΔJ_3 with the fixed density 0.91×10^3 kg m^{-3} (Smith et al., 2001). It agrees fairly well with the gravimetric ΔJ_3, but the disagreements appear largely systematic, e.g. gravimetric ΔJ_3 are continuously larger than altimetric ΔJ_3 after $L_s \sim 180°$ but this reverses at $L_s \sim 240°$. Next we will show that such disagreements come from the wrong assumption of constant snow density.

2.2. Time–variable snow density

Terrestrial H_2O snow usually changes its density seasonally, i.e. it starts with a small density as freshly fallen snow, and gradually becomes denser by compaction due to its own mass as it thickens.

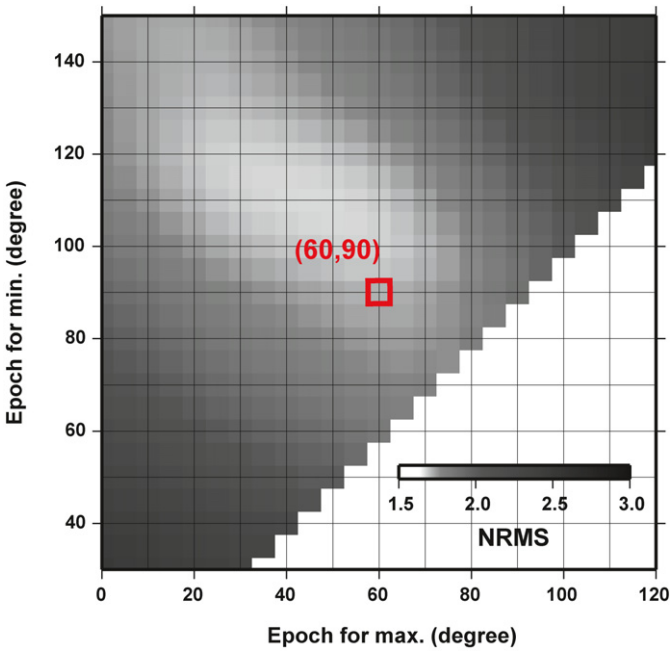

Fig. 3. Variation of NRMS between the gravimetric and altimetric ΔJ_3 by assuming different epochs (in L_s) for the maximum and minimum average densities of snow packs. Brighter colors show better fits. Here, the search was performed in 5 degree steps with the model 3 (red curve in Fig. 2). We adopted 60° ($t_{\max}$) and 90° (t_0) to draw Fig. 2. (For interpretation of the references to color in this figure legend, the reader is referred to the web version of this article.)

It is due partly to sintering, combining of solid crystals that occur when temperatures approach the melting points. Heki (2004) suggested that such increase is often nearly linear in time. Here we assume that similar compaction occurs on Mars, and allow the density ρ_{snow} to increase (model 2). Then, the snow density obeys

$$\rho_{\mathrm{snow}}(t) = \rho_0 + \alpha(t - t_0), \quad (3)$$

where ρ_0 is the density of fresh snow that starts to accumulate at time t_0, and α is the increasing rate. Instead of estimating the parameter α, we rewrite ρ_{snow} using the maximum density $\rho_{\max}$ which is achieved at time $t_{\max}$, i.e.

$$\rho_{\mathrm{snow}}(t) = \frac{t_{\max} - t}{t_{\max} - t_0}\rho_0 + \frac{t - t_0}{t_{\max} - t_0}\rho_{\max} \quad (t_0 < t < t_{\max}). \quad (4)$$

First, we assume that ρ_0 and $\rho_{\max}$ take same values every winter, and estimate them by least-squares method to minimize the differences between the gravimetric and altimetric ΔJ_3. We used the error of ΔJ_3 given by Konopliv et al. (2006) to weight individual data. The values of t_0 and $t_{\max}$ are determined by grid search so that the smallest post-fit residuals are achieved (Fig. 3).

The result drawn in green in Fig. 2 shows a much improved fit (post-fit residual significantly decreased, see Fig. 2 inset), suggesting that the compaction of the martian snow does occur. The current data set is not sensitive enough to ρ_0, the density of fresh snow, to accurately constrain it because the thin early snow little disturbs the gravity field. Hence we stabilized the least-squares estimation by constraining ρ_0 around its a-priori value 100 kg m^{-3} as strongly as ±30 kg m^{-3}. Actually, the fit does not vary significantly for a range of realistic values of ρ_0.

In the northern hemisphere, we took $t_{\max}$ and t_0 at 60° and 90° in the solar longitude L_s, respectively (240° and 270° in the southern hemisphere), as determined by grid search (Fig. 3). These L_s correspond to the ends of May and June in the Earth, respectively. We set up two epochs and let the density decrease from $\rho_{\max}$ to ρ_0 over a finite duration because this resulted in a better fit than instantaneous density drop (i.e. $t_{\max}$ and t_0 are infinitely close).

This may reflect the diversity of the "crocus day" (the day when old snows disappear) at places with different latitudes and sunlight conditions. Although transitions from old to new snow may occur in one epoch at individual places, hemispheric average apparently shows such two-epoch behavior. The average of these two epochs is fairly well constrained at ~75°, but their separation is only weakly constrained as seen in the diagonally right down pattern of the bright part in Fig. 3 (i.e. 50°/100° combination provides almost as good fit as 60°/90°). Here we plot the results assuming the 60°/90° pair assuming tentatively that the thawing takes ~30 degrees in solar longitude (~1 month).

2.3. Difference between winters

Next, we allowed the maximum snow density ρ_{max} to take different values in different winters and hemispheres (model 3), and performed the least-squares estimation for four parameters in total (one northern winter and two southern winters, plus the initial density). The normalized root-mean-square of ΔJ_3 significantly decreased again (Fig. 2 inset). We obtained similar ρ_{max} in the first southern winter, $(1.22 \pm 0.05) \times 10^3$ kg m^{-3}, and in the northern winter, $(1.15 \pm 0.07) \times 10^3$ kg m^{-3}. However, the value for the second southern winter was significantly larger, i.e. $(1.64 \pm 0.07) \times 10^3$ kg m^{-3} at the end of the data set ($L_s = 525$).

The snow density in the second southern winter is larger than the solid CO_2 (~1.5×10^3 kg m^{-3}), which may reflect multiple causes. One possibility is the influence of dust storms and dust particles incorporated into the snow pack. Dust storms occur more frequently when Mars is near its perihelion (Smith, 2004), and this period corresponds to spring-summer in the southern hemisphere. The two largest dust storms in the studied period occurred when L_s was between 225° and 285° (Fig. 2) (Smith, 2004), and the second one (L_s: 270°–285°) occurred in the south polar region when the CO_2 snow in the previous winter started to be replaced by the new one. This storm may have increased the snow density by putting silicate dust particles into the growing snow-cap. However, in order to bring snow pack of 1.0×10^3 kg m^{-3} to 1.6×10^3 kg m^{-3}, we need ~30% of dust (2.9×10^3 kg m^{-3}) and this seems too large to be real. Additional density increase might have come from enhanced sintering of the snow pack by, e.g. temporary warming by the storm or modification of physical properties of the snow pack by including dust particles.

3. Sources of error

In addition to the observation errors and the systematic overestimation of snow density due to the negligence of snow distribution expressed in higher degree zonal spherical harmonics (see Section 2.1), a few factors may influence the estimation of the martian snow density. For example, two factors, i.e. redistribution of atmospheric mass, and deformation of the martian equipotential surface (Areoid) due to ice load, affect gravimetric ΔJ_3. Additionally, deformation of the martian surface due to snow load, affects altimetric ΔJ_3.

Evaluation of the ΔJ_3 due to atmospheric mass redistribution is straightforward; we can calculate it with Eq. (2) substituting snow masses with those of atmosphere. We used half-monthly snapshots of martian atmospheric pressure distribution available in the Planetary Data System Geosciences Node (http://pds-geosciences.wustl.edu/). The root-mean-squares of the atmospheric ΔJ_3 in the studied period was $\sim 0.14 \times 10^{-9}$, which is ~5% of those by snow. Because its temporal changes are fairly random, it would little influence our conclusion. Seasonal exchange of CO_2 between the atmosphere and polar caps could also contribute to the seasonal change of gravity coefficients because atmospheric mass distribution is not uniform due to non-flat Areoid surface. Chao and Rubincam (1990) found that it could influence ΔJ_2, but its contribution to ΔJ_3 is negligible.

Changes of the martian snow load cause elastic deformation of the planet, and secondary changes of gravity (or Areoid height). For example, thick and heavy snow depresses the crust, and the redistributed mass in the martian interior modifies its gravity signature (ΔJ_3 in this case), i.e.

$$\Delta J_3^{\mathrm{Obs}} = \Delta J_3^{\mathrm{True}}\left(1 + k_3^l\right). \tag{5}$$

There k_3^l is the martian load Love number of degree 3 for gravity, and $\Delta J_3^{\mathrm{True}}$ is the value to be observed if Mars is perfectly rigid. Normally, k_3^l is negative (the deformation reduces the amplitude of J_3 changes), and is about −0.194 for the Earth (Han and Wahr, 1995). Although it has never been measured for Mars, we have good reasons to consider it significantly smaller than the Earth. From Doppler shift observations of MGS, Yoder et al. (2003) suggested that the martian tidal Love number of degree 2 (k_2^t) is ~0.15. This is nearly a half of k_2^t of the Earth. Métivier et al. (2008) calculated the martian load Love numbers assuming a plausible internal structure with a liquid outer core. There k_3^l is inferred to be between −0.05 and −0.08. Thus, the elastic deformation of Mars due to surface load might cause systematic underestimation of ΔJ_3 (and snow density, too). However, it would not exceed 10%, and this would partly cancel the overestimation of the snow density by neglecting coefficients with degrees >9 in calculating altimetric ΔJ_3.

Martian surface deformation due to snow load might also affect snow depth measurements by MOLA. Because the snow depresses the martian surface, the orbital laser altimeter may underestimate the true snow depth. The relationship between vertical displacement Δu and the observed ΔJ_3 is

$$\Delta u(\theta) = R\left(\frac{h_3^l}{1 + k_3^l}\right)\Delta J_3^{\mathrm{Obs}} \bar{P}_{3,0}(\sin\theta), \tag{6}$$

where $P_{3,0}(\sin\theta)$ is the normalized spherical harmonics with degree 3 and order 0, and θ is the latitude (e.g., Davis et al., 2004). There h_3^l is the load Love number of degree 3 for vertical, and Métivier et al. (2008) suggested it to be between −0.21 and −0.30. Thus Δu would remain smaller than a centimeter under the observed amplitudes of ΔJ_3. This is much smaller than the elevation errors (Smith et al., 2001), and would not influence our conclusion.

Systematic error in MOLA data due to orbital uncertainty could also cause errors in snow density. MOLA data in Smith et al. (2001) show that the maximum elevation change is slightly more than 1 m in the north and slightly less than 1 m in the south. Aharonson et al. (2004) reprocessed the MOLA crossover data at latitudes 86° north and south, and showed that the snow depth variation reach ~1.5 m in the north and ~2.5 m in the south, values much larger and more asymmetric than Smith et al. (2001). Here we see how this revision may influence our results.

First we extrapolated the snow depth data at 86° north/south (Aharonson et al., 2004) to lower latitude regions assuming that the depth linearly decreases to zero at 65°. We then followed the same procedure as in Section 2, and obtained ρ_{max} of $(0.44 \pm 0.05) \times 10^3$, $(0.56 \pm 0.1) \times 10^3$, and $(0.61 \pm 0.01) \times 10^3$ kg m^{-3} for the first southern winter, the northern winter, and the second southern winter (the value at the end of the data set, i.e. $L_s = 525$), respectively. Although the absolute values of the density decreased by half, the essence of the present study remains the same, i.e. density increase toward the end of winter and the larger density in the second southern winter. In fact, time–variable density gives much better fit than the constant density of 0.5×10^3 kg m^{-3} given by Aharonson et al. (2004).

4. Conclusion

We compared the gravimetric ΔJ_3, observed by Doppler tracking, and altimetric ΔJ_3, inferred from the snow depth measured by MOLA, and estimated the average volume density of the snow pack. In doing so, we found that they agree better by allowing the snow density to increase in time, i.e. freshly sublimated light snow gets denser until it thaw in late spring and early summer. From analogy to terrestrial H_2O snow (Maeno and Kuroda, 1986), we suggest possible densification mechanisms such as gravity-driven compaction and/or sintering of CO_2 crystals.

Next we discussed the difference in the maximum snow densities among the three winters. The second southern winter showed maximum density significantly larger than the others. We speculate that it reflects dust storm activities during the growth of the snow pack, i.e. incorporation of significant amount of dust particles into snow, and enhanced sintering related to dust storms. Evaluation of systematic errors caused by elastic deformation of Mars and by the neglect of snow distribution expressed by spherical harmonics of degrees >10, suggested that the obtained snow density might be overestimated by 10% (or a little more) in total. As suggested by revised estimate of snow depth by Aharonson et al. (2004), improved measurements of snow depths in future Mars exploration missions may call for major modifications of absolute values of the density.

Acknowledgments

We thank Alex Konopliv, JPL, for sending gravity data, Sander Goossens, NAO, for comments, and Akira Kouchi and Masatsugu Odaka, Hokkaido University, Ben Chao, National Central University, Taiwan, for their advises on martian snow and atmosphere. Critical reviews by two anonymous referees also improved the manuscript.

References

Aharonson, O., Zuber, M.T., Smith, D.E., Neumann, G.A., Feldman, W.C., Prettyman, T.H., 2004. Depth, distribution, and density of CO_2 deposition on Mars. J. Geophys. Res. 109, doi:10.1029/2003JE002223. E05004.

Chao, B.F., Rubincam, D.P., 1990. Variations of Mars gravitational field and rotation due to seasonal CO_2 exchange. J. Geophys. Res. 95, 14755–14760.

Davis, J.L., Eloségui, P., Mitrovica, J.X., Tamisiea, M.E., 2004. Climate-driven deformation of the solid Earth from GRACE and GPS. Geophys. Res. Lett. 31, doi:10.1029/2004GL021435. L24605.

Feldman, W.C., Prettyman, T.H., Boynton, W.V., Murphy, J.R., Squyres, S., Karunatillake, S., Maurice, S., Tokar, R.L., McKinney, G.W., Hamara, D.K., Kelly, N., Kerry, K., 2003. CO_2 frost cap thickness on Mars during northern winter and spring. J. Geophys. Res. 108, doi:10.1029/2003JE002101. 5103.

Han, D., Wahr, J., 1995. The viscoelastic relaxation of a realistically stratified Earth, and a further analysis of post glacial rebound. Geophys. J. Int. 120, 287–311.

Heki, K., 2004. Dense GPS array as a new sensor of seasonal changes of surface loads. In: Sparks, R.S.J., Hawkesworth, C.J. (Eds.), The State of the Planet: Frontiers and Challenges in Geophysics. In: Geophys. Monographs, vol. 150. Am. Geophys. Union, Washington, pp. 177–196.

Konopliv, A.S., Yoder, C.F., Standish, E.M., Yuan, D.-N., Sjogren, W.L., 2006. A global solution for the Mars static and seasonal gravity, Mars orientation, Phobos and Deimos masses, and Mars ephemeris. Icarus 182, 23–50.

Maeno, N., Kuroda, T., 1986. Structure and Physical Properties of Ice and Snow. Series of Basic Glaciology, vol. 1. Kokon-Shoin, Tokyo, Japan, p. 212 (in Japanese).

Métivier, L., Karatekin, Ö., Dehant, V., 2008. The effect of the internal structure of Mars on its seasonal loading deformations. Icarus 194, 476–486.

Smith, M.D., 2004. Interannual variability in TES atmospheric observations of Mars during 1999–2003. Icarus 167, 148–165.

Smith, D.E., Zuber, M.T., Neumann, G.A., 2001. Seasonal variation of snow depth on Mars. Science 294, 2141–2146.

Wahr, J., Molenaar, M., Bryan, F., 1998. Time variability of the Earth's gravity field: Hydrological and oceanic effects and their possible detection using GRACE. J. Geophys. Res. 103, 30205–30229.

Yoder, C.F., Konopliv, A.S., Yuan, D.N., Standish, E.M., Folkner, W.M., 2003. Fluid core size of Mars from detection of the solar tide. Science 300, 299–303.